**International Journal of Applied Mathematics**
**Volume 38 No. 4s, 2025**
ISSN: 1311-1728 (printed version); ISSN: 1314-8060 (on-line version)

# DEEP LEARNING APPROACHES FOR EARLY DETECTION OF SKIN CANCER

Mihika Pandit[1], Sandhya Arora[2], Saniya Mahalle[3], Srushti Pekamwar[4], Vaishnavi Rohokale[5]
[1]MKSSS's Cummins College of Engineering for Women, Pune, INDIA
email: mihikapandit1@gmail.com,
[2]MKSSS's Cummins College of Engineering for Women, Pune, INDIA
email: sandhya.arora@cumminscollege.in
[3]MKSSS's Cummins College of Engineering for Women, Pune, INDIA
email: saniya.mahalle@gmail.com,
[4] MKSSS's Cummins College of Engineering for Women, Pune, INDIA
email: srushtipekamwar@gmail.com,
[5]MKSSS's Cummins College of Engineering for Women, Pune, INDIA
email: rohokalevaishnaviraju123@gmail.com

**Abstract:** Melanoma is one of the most aggressive skin cancer types and is notorious for rapid progression, highlighting the necessity of early detection to increase survival outcomes. The conventional diagnostic process can be invasive, consumes too much time, and is relatively dependent on professional evaluation. In this study, the following deep learning models are evaluated: VGG19, DenseNet121, InceptionV3, and EfficientNetB1 with various datasets such as HAM10000, PAD-UFES-20, and ISIC 2016. The deep learning models are evaluated as a function of accuracy and ROC-AUC metrics, with consideration of other problems such as class imbalance, computational performance, and model complexity. The study discusses processes for data augmentation, efficient image processing, as well as ways to incorporate clinical aspects, which could increase the accuracy of skin cancer diagnosis by deep learning models. Future work consists of investigating efficient lightweight models and conducting clinical evaluations to allow real-world applications.

**Math. Subj. Classification 2020:** 68T01, 68T05, 68T07
**Keywords:** Skin cancer, Deep learning, VGG19, DenseNet121, InceptionV3, EfficientNetB1

## I. Introduction

The skin is the body's first line of protection, limiting exposure to UV radiation, toxins, and bacteria. Cancer is one of the biggest threats to the skin. Melanoma is the deadliest form of skin cancer because it is very aggressive in its growth and ability to spread in the body. Skin cancer cases are increasing all across the world and are increasingly diagnosed at younger ages, which is largely due to UV damage resulting from the depletion of the ozone layer. Melanoma is the 17th most prevalent cancer in the world, but has the highest occurrence in Europe and the highest mortality in Asia. Oceania, which includes Australia and New Zealand, has the highest incidence because of its high UV exposure and fair-skinned population. [1-4]

Early diagnosis is key to improving outcomes, but existing diagnosis methods (such as dermoscopy and biopsy) are invasive, slow, and require pathology specialists. This drives the need for new non-invasive, efficient, and accurate diagnostic procedures to distinguish between malignant and benign lesions. The skin cancer detection process typically involves obtaining an

Received: July 25, 2025

Volume 38 No. 4s, 2025
ISSN: 1311-1728 (printed version); ISSN: 1314-8060 (on-line version)

image, preprocessing the image, segmenting the image, extracting image features, and classifying the image. Recently, deep learning, particularly convolutional neural networks (CNNs), has shown exceptional performance in medical imaging tasks and dermatological diagnosis. Different CNNs have also been successfully presented to accurately extract the complicated features of lesions, and therefore, increase the detection accuracy for skin cancers.

## II. Literature Review

Deep learning has significantly advanced skin cancer detection, with models like DenseNet, InceptionNet, VGG, ResNet, Xception, EfficientNet, U-Net, and Vision Transformers actively explored in research. Each architecture brings unique strengths: ResNet excels in deep training, Xception and MobileNet support real-time efficiency, U-Net is ideal for segmentation tasks, and Vision Transformers effectively capture intricate patterns. Generative Adversarial Networks (GANs) address data scarcity by producing synthetic images. Contemporary strategies also include transfer learning, data augmentation, and incorporating clinical data to improve model performance and real-world applicability. In this study, VGG19, InceptionV3, DenseNet121, and EfficientNetB1 are the primary models under evaluation.

**VGG19:** In [15], the authors proposed a new version of VGG19 to detect skin cancer on the HAM10000 dataset through (i) eliminating the convolutional layer in the third block, (ii) using batch normalization (BN) instead of dropout, (iii) using BN again after the pooling layer, and (iv) replacing the fully connected layers with Global Average Pooling (GAP). They fine-tuned all layers and achieved testing accuracy of 82%. One limitation of this study is that it is performed on only one dataset. In [16], a VGG19 model trained on the ISIC archive achieved an accuracy of 87%, compared with VGG16 and Inception models, but their architectural improvements were not included.

**InceptionV3:** Similarly, Bazgir et al. [18] employed InceptionV3 with transfer learning and data augmentation to predict skin lesions, with 84.39% and 85.94% accuracy using Adam and Nadam optimizers, respectively. Although effective, they did not report performance metrics such as sensitivity and specificity and also did not solve class imbalance. Alanazi et al. [19] employed InceptionV3 on the ISIC dataset, employing Gaussian filters for denoising and bottleneck features for computational efficiency. They attained 98.96% with transfer learning but, similar to Bazgir et al., lacked thorough analyses and generalizability across various populations.

**DenseNet121:** In [21] the study leverages DenseNet architectures as baseline models for the classification of skin lesions. The research utilized the ISIC 2018 dataset. This model was fine-tuned by employing different data augmentation techniques like random cropping, Gaussian blur, and the addition of salt and pepper noise, and it achieved an accuracy of 81.5%. In [22] DenseNet121 was used as one of the models in the proposed model. Global average pooling was used to reduce the number of model parameters and softmax activation was used for classification. The research utilized the ISIC 2018 dataset. An accuracy of 91% was achieved by the authors.

Received: July 25, 2025

**International Journal of Applied Mathematics**
**Volume 38 No. 4s, 2025**
ISSN: 1311-1728 (printed version); ISSN: 1314-8060 (on-line version)

**EfficientNetB1:** Amin Tajerian et al. (2023) [23] utilized the EfficientNetB1 model to classify skin cancer images from the HAM10000 dataset, achieving 84.3% accuracy. Their model structure included a global pooling 2D layer and a 7-node softmax layer. However, limitations such as restricted geographic diversity and unaddressed class imbalance affect its generalization. Kanchana K et al. [24] also applied EfficientNetB1 with transfer learning from ImageNet and incorporated preprocessing methods like augmentation and noise reduction.This achieved 82.5% top-1 accuracy but struggled with class imbalance. Irfan Ullah Khan et al. [25] used EfficientNetB3 with PAD-UFES-20 dataset, enhancing it with GlobalAveragePooling2D layer and transfer learning. This model achieved 76% accuracyand F1 score of 0.81,but still struggles with data imbalance and need for validation on multiple datasets remain.

**Table 1: A literature review of various deep learning Models**

| Author | Title | Technique | Limitations |
|---|---|---|---|
| Irfan Ali Kandhro et al. [5] | Performance evaluation of E-VGG19 model: Enhancing real-time skin cancer detection and classification | Enhances the **VGG19** pre-trained model by using the HAM10000 dataset with 82% testing accuracy | Limited dataset usage |
| Kiran Likhar, Dr.Sonali Ridhorkar [6] | Enhancing Skin Cancer Detection: A Comparative Analysis of Models with VGG-16, VGG-19, and Inception V3 | Used the **E-VGG19** on the ISIC archive dataset with 87% testing accuracy | Limited exploration of a broader range of models |
| Bansal, M.et al. [7] | Transfer learning for image classification using VGG19: Caltech-101 image data set | Implemented the **VGG19** model along with **Gaussian Naïve Bayes** classifier with 92.05% testing accuracy | Limited scope of classifiers |
| Ehsan Bazgir et al. [8] | Skin Cancer Classification using Inception Network | Achieved 84.39% and 85.94% accuracy with **InceptionV3** using Adam and Nadam, respectively on the ISIC dataset | Did not address class imbalance |

Received: July 25, 2025

Volume 38 No. 4s, 2025
ISSN: 1311-1728 (printed version); ISSN: 1314-8060 (on-line version)

| | | | |
|---|---|---|---|
| Alanazi et al. [9] | Melanoma Identification Through X-ray Modality Using Inception-v3 Based Convolutional Neural Network | Applied the **InceptionV3** model with transfer learning and Gaussian filters for skin cancer diagnosis, achieving 98.96% accuracy | Lacked broader evaluation across diverse populations |
| Bhavya Sai et al. [10] | Classification of skin cancer images using TensorFlow and inception v3 | Achieved over 85% accuracy using **InceptionV3** with bottleneck feature extraction, optimized for CPU-based efficiency | Did not address class imbalance |
| Rashid H, Asjid Tanveer M, Khan HA [11] | Skin Lesion Classification Using GAN-based Data Augmentation | Achieved accuracy of 81.5% using **DenseNet** by employing various data augmentation techniques | Limited datasets usage (ISIC 2018 dataset) |
| Alfi IA, Rahman MM, Shorfuzzaman M, Nazir A [12] | A Non-Invasive Interpretable Diagnosis of Melanoma Skin Cancer Using Deep Learning and Ensemble Stacking of Machine Learning Models | Achieved accuracy of 91% using **DenseNet121** | Limited datasets usage (ISIC 2018 dataset) |
| Amin Tajerian et al. [13] | Design and validation of a new machine-learning-based diagnostic tool for the differentiation of dermatoscopic skin cancer images | Developed a web application for classifying skin cancer lesions of the HAM10000 dataset with the **EfficientNet-B1** model and shows an **accuracy of 84.3%** on the test set. | Imbalanced class distribution, with a predominance of melanocytic nevi images, potential for overfitting |
| Kanchana K et al. [14] | Enhancing Skin Cancer Classification Using Efficient Net B0-B7 through Convolutional Neural Networks and Transfer Learning with Patient-Specific Data | The **EfficientNetB1** model achieved a **top-1 accuracy of 82.5%** and a top-5 accuracy of 89.5% on the ISBI dataset, which is a subset of the ISIC Archive | Did not address the class imbalance and lack of Generalization across diverse Skin Lesions |

Received: July 25, 2025

International Journal of Applied Mathematics
Volume 38 No. 4s, 2025
ISSN: 1311-1728 (printed version); ISSN: 1314-8060 (on-line version)

## III. Methodology

To address binary skin cancer classification, four models of deep learning—VGG19, InceptionV3, DenseNet121, and EfficientNetB1—were trained, tested, and assessed using three datasets (HAM10000, ISIC2016, and PAD-UFES-20). This organized comparison gave understanding of each model's real-world efficiency. As evident from the system architecture diagram, input images of the datasets are taken by the pre-trained models, which classify every image as Malignant or Benign.

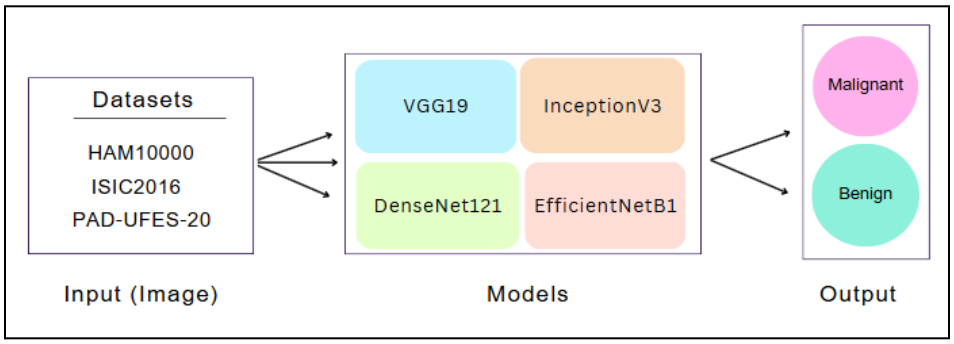


**Fig.1 Comprehensive System Architecture Diagram**

This diagram illustrates a process for skin cancer detection using deep learning models. It shows that images from different datasets, specifically **HAM10000**, **ISIC2016**, and **PAD-UFES-20**, serve as input. These images are fed into a set of pre-trained deep-learning models: **VGG19**, **InceptionV3**, **DenseNet121**, and **EfficientNetB1**. The models then analyze the input images to produce an output that classifies the images as either **Malignant** or **Benign**. The diagram highlights the flow from image data input through model processing to the final classification output.

### A) Datasets:

Three public datasets—PAD-UFES, ISIC 2016, and HAM10000—were utilized, all with labeled images of benign and malignant lesions. HAM10000 contains 10,015 images divided into seven categories with a benign slant. ISIC 2016 has 1,279 images concentrated on melanoma detection with an indication of class imbalance. PAD-UFES has 2,298 images of six lesion types with fewer imbalances than the other two. Figure 2 shows sample images from the datasets.

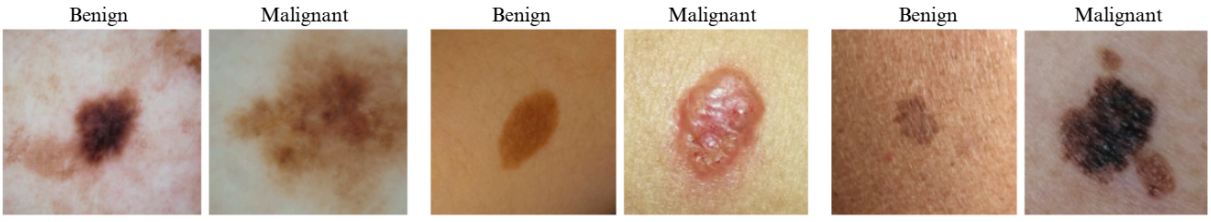


a) HAM10000 b) ISIC 2016 c) PAD-UFES-20

Received: July 25, 2025

**International Journal of Applied Mathematics**
**Volume 38 No. 4s, 2025**
ISSN: 1311-1728 (printed version); ISSN: 1314-8060 (on-line version)

**Figure 2: Example Images from Datasets**

Malignant categories were underrepresented, particularly in HAM10000 and ISIC 2016. To resample the datasets, we utilized oversampling and data augmentation methods such as rotation, flipping, brightness adjustments, cropping, and zooming. This, as indicated in Figure 3, balanced classes and enhanced model performance and decreased bias.

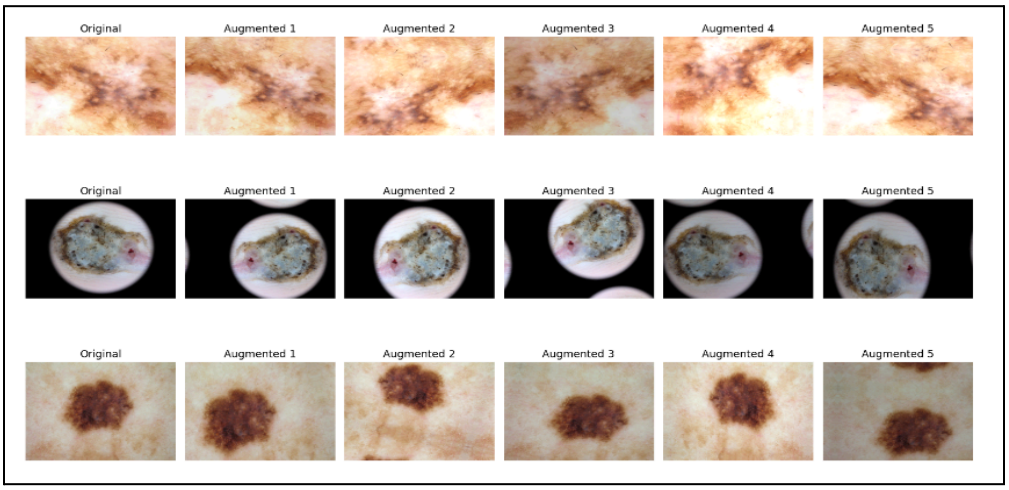


**Figure 3: Images before and after augmentation**

**B) Models:**

1. **VGG19**:

This study uses VGG19, a deep CNN with 19 layers (16 convolutional layers, 3 fully connected layers) due to its simple structure and efficiency of utilizing a set of 3×3 filters. The model has been pre-trained on ImageNet, allowing us to take advantage of the low-level features before we fine-tuned the model to the binary classification task by simply changing the last layer. We also added a Global Average Pooling (GAP) layer then a dense layer with 512 neurons to increase the features being learned. VGG19 utilizes the Adam optimizer, cross-entropy loss function, early stopping, selected neurons with sigmoid activation to prevent overfitting, and provides an output for binary classification, while VGG19 requires very high computing power due to its depth in architecture, as can be seen in Fig. 4.

Received: July 25, 2025

**International Journal of Applied Mathematics**
**Volume 38 No. 4s, 2025**
ISSN: 1311-1728 (printed version); ISSN: 1314-8060 (on-line version)

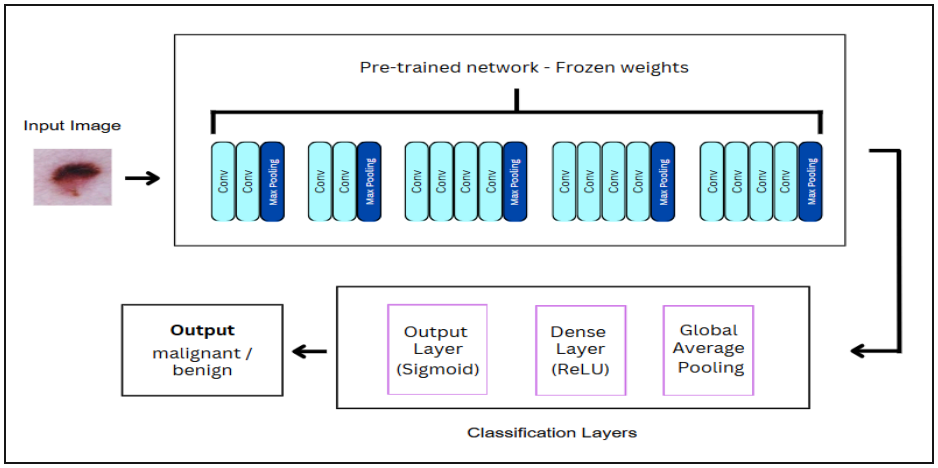


**Figure 4: VGG19 Architecture**

## 2. InceptionV3:

InceptionV3 was used in this work for binary classification as it is efficient and can learn hierarchical features. Pre-trained on ImageNet, the network used acquired features such as edge and texture detection, and the default classifier was replaced for binary classification. Input RGB images were resized to 299×299×3 to be compatible with the architecture. The structure of InceptionV3, which uses convolutional, pooling, and Inception modules, extracts both low-level and high-level features. Its application of multiple filter sizes (e.g., 1×1, 3×3, 5×5) in Inception modules allows multi-scale feature detection, essential in identifying minute differences in skin lesions. A special architecture was stacked on top of the InceptionV3 base, with a Global Average Pooling (GAP) layer used to decrease feature dimensionality. A dense layer of 1,024 neurons and ReLU activation was employed to learn intricate patterns, and then a sigmoid output layer for binary classification. Training was initiated by freezing the base layers, and then fine-tuning the whole model. Early stopping was used to avoid overfitting.

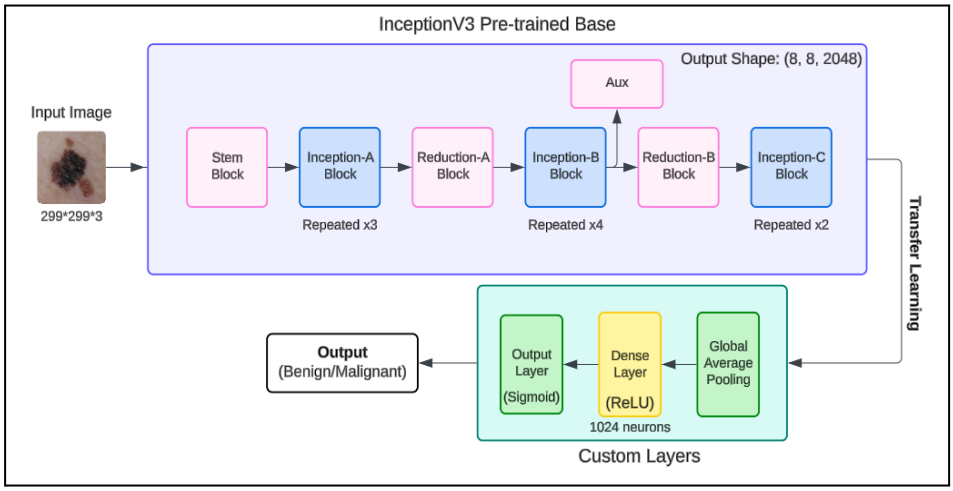


**Figure 5: InceptionV3 Architecture**

Received: July 25, 2025

**International Journal of Applied Mathematics**
**Volume 38 No. 4s, 2025**
ISSN: 1311-1728 (printed version); ISSN: 1314-8060 (on-line version)

### 3. DenseNet121:

DenseNet121 due to its dense connections, enhances feature propagation and gradient flow by allowing each layer to receive inputs from all previous layers which makes it effective for image classification. For binary skin lesion classification, a pre-trained DenseNet121 model is used with transfer learning. The input images are resized to (224, 224, 3) and normalized to [0, 1], and then these images are passed through dense and transition layers. The dense blocks capture hierarchical features and the transition layers reduce spatial dimensions and feature maps. After feature extraction is done by the base model, a global average pooling layer converts 2D feature maps into 1D vectors. 50% dropout is applied to prevent overfitting. A fully connected layer with 1024 ReLU-activated units is used to learn high-level features and then the output layer predicts the probability of whether the lesion being benign or malignant using sigmoid activation function. Figure 6 illustrates the DenseNet121 architecture.

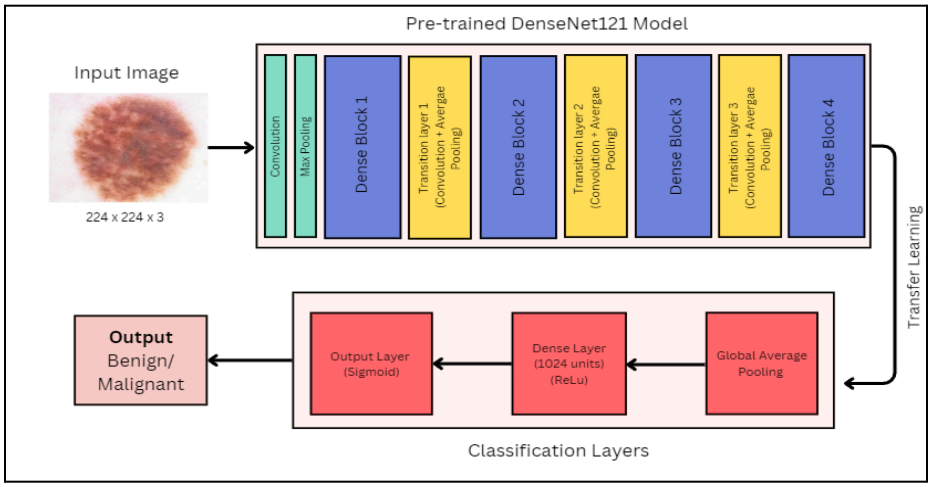


**Figure 6: DenseNet121 Architecture**

### 4. EfficientNetB1:

This study uses the EfficientNetb1 model for its balance of efficiency and lower hardware demands. Input images(240X240) pass through a pre-trained network with frozen weights, featuring MBConv blocks,swish activation, and batch normalization. After global average pooling, features are flattened and passed to custom classifier layers, including a dense layer with 512 units(ReLU) and dropout, and a final sigmoid-activated output for binary classification. Figure 7 shows the architecture.

Received: July 25, 2025

**International Journal of Applied Mathematics**
**Volume 38 No. 4s, 2025**
ISSN: 1311-1728 (printed version); ISSN: 1314-8060 (on-line version)

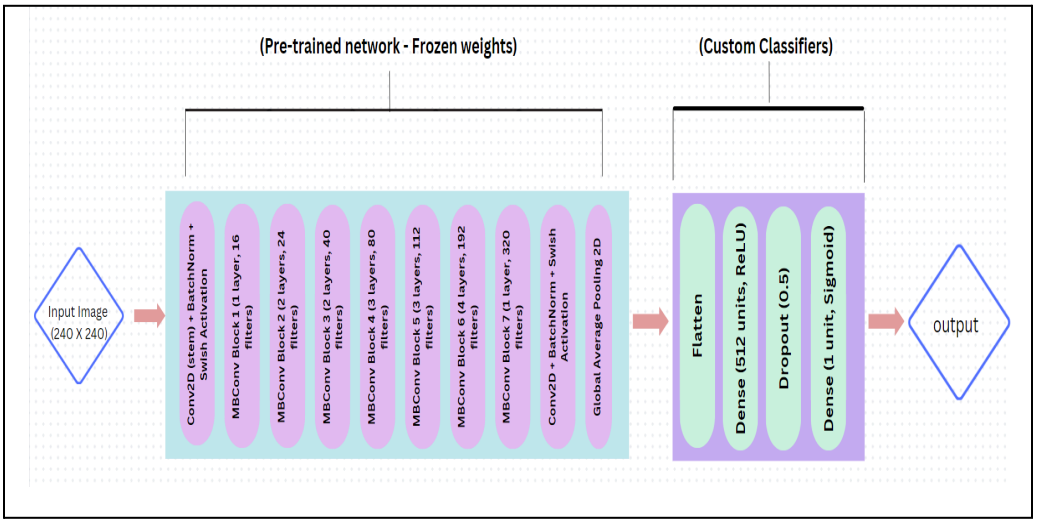


**Figure 7. EfficientNetB1 Architectural Diagram**

## IV. Results:

The performance of various deep learning models was evaluated for the binary classification of skin cancer using three datasets: HAM10000, ISIC, and PAD-UFES.

### VGG19:

The VGG19 model shows good performance on the HAM10000, ISIC 2016, and the PAD-UFES-20 datasets. The accuracy on HAM10000 was 87.39% with a ROC of 0.88, which suggests that the results were relatively balanced. The ISIC 2016 dataset yielded a relative effectiveness of 79.95 and an ROC of 0.73. However, the PAD-UFES-20 dataset resulted in a sharp drop, with accuracy at 60.65% and ROC of 0.46, which implies issues with generalization. Throughout the data sets, it is evident that the VGG19 model works really well on the HAM10000 and ISIC 2016 datasets but seems to struggle when exposed to the subsequent datasets, suggesting the model does not have an appropriate vis-à-vis adaptability when switching datasets/conditions. The confusion matrix and ROC curves are shown in Figures 8-10 for all datasets.

Received: July 25, 2025

**International Journal of Applied Mathematics**
**Volume 38 No. 4s, 2025**
ISSN: 1311-1728 (printed version); ISSN: 1314-8060 (on-line version)

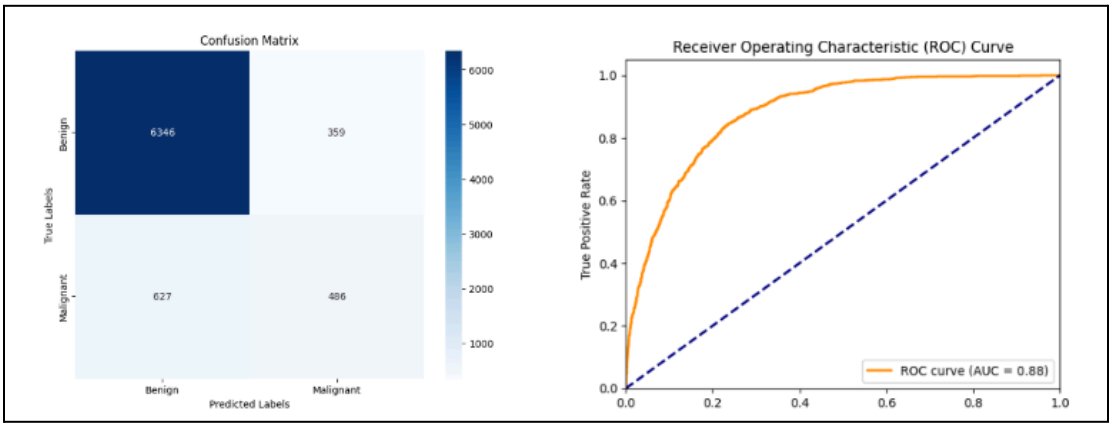


**Figure 8. VGG19 Results on HAM10000 Dataset**

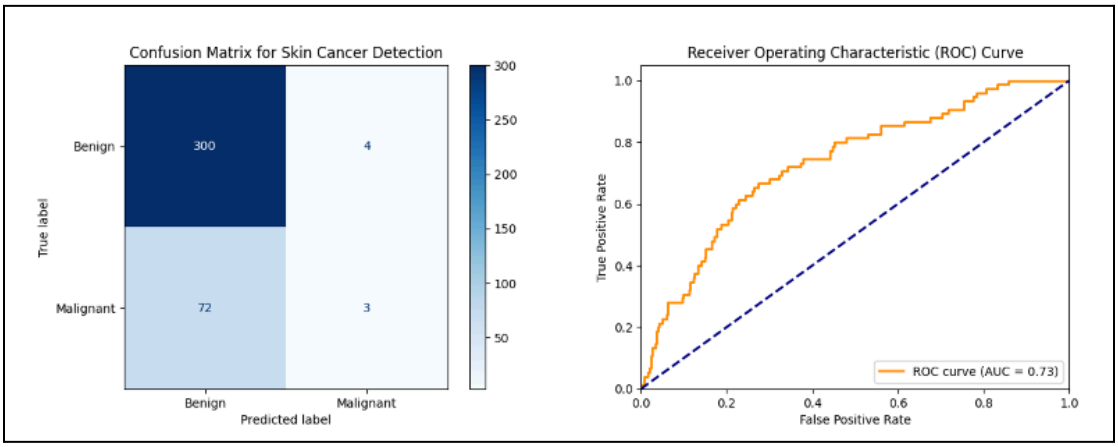


**Figure 9. VGG19 Results on ISIC 2016 Dataset**

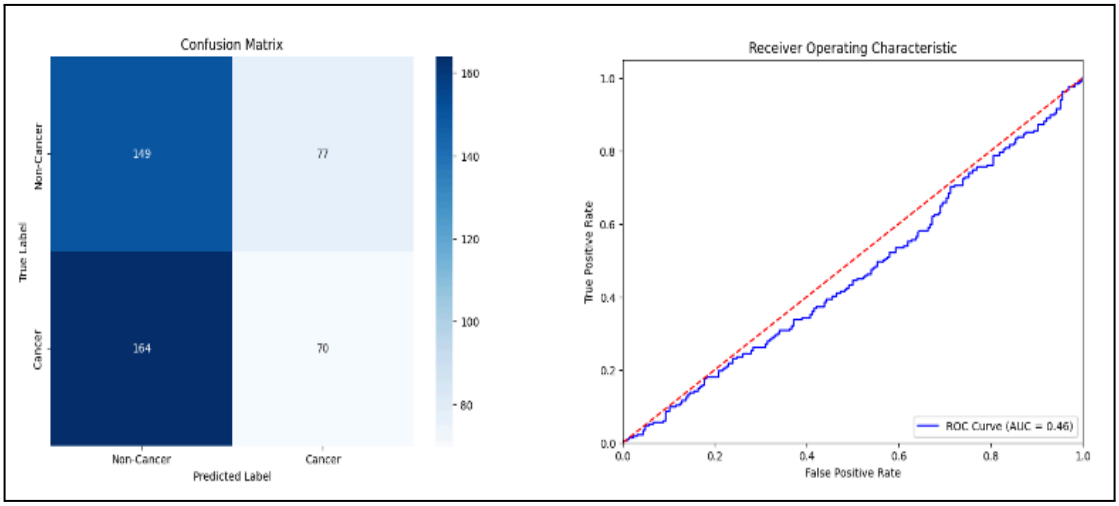


**Figure 10. VGG19 Results on PAD-UFES-20 Dataset**

Received: July 25, 2025

International Journal of Applied Mathematics
Volume 38 No. 4s, 2025
ISSN: 1311-1728 (printed version); ISSN: 1314-8060 (on-line version)

## InceptionV3:

The model's performance was moderate with an accuracy rate of 69.24% and ROC-AUC of 0.63 on the HAM10000. These results suggest that while the model is moderately effective, it struggles with precise discrimination. It struggles to capture the complex features within the dataset images. In contrast, the results of the ISIC dataset were favorable since the model could perform well and obtain 83.64% accuracy and ROC-AUC of 0.79. In the case of the PAD-UFES dataset, the model yielded 73.26% accuracy, but the overall ROC-AUC dropped to 0.51. This indicates that while dataset balancing helped alleviate any class imbalance concerns, factors such as noise or less distinguishable features present in the dataset led to a lesser overall discriminative efficacy. Figures 11, 12, and 13 display the ROC curves and confusion matrix for the InceptionV3 model.

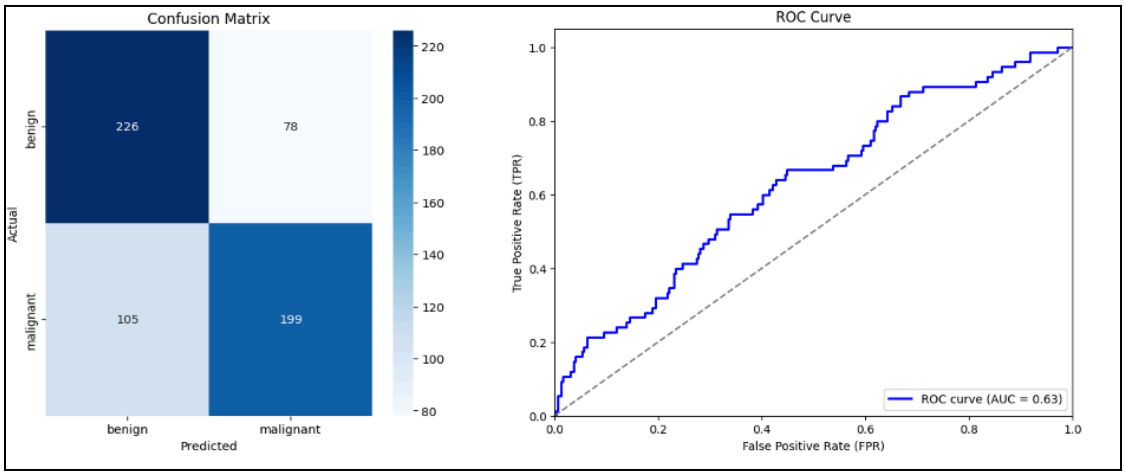


**Figure 11: InceptionV3 Results on HAM10000 Dataset**

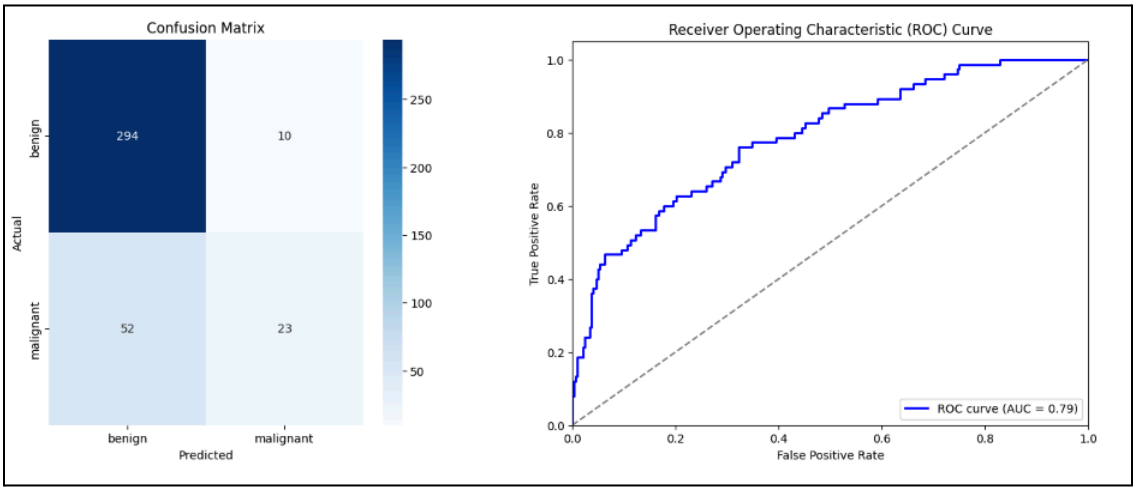


**Figure 12: InceptionV3 Results on ISIC 2016 Dataset**

Received: July 25, 2025

Volume 38 No. 4s, 2025
ISSN: 1311-1728 (printed version); ISSN: 1314-8060 (on-line version)

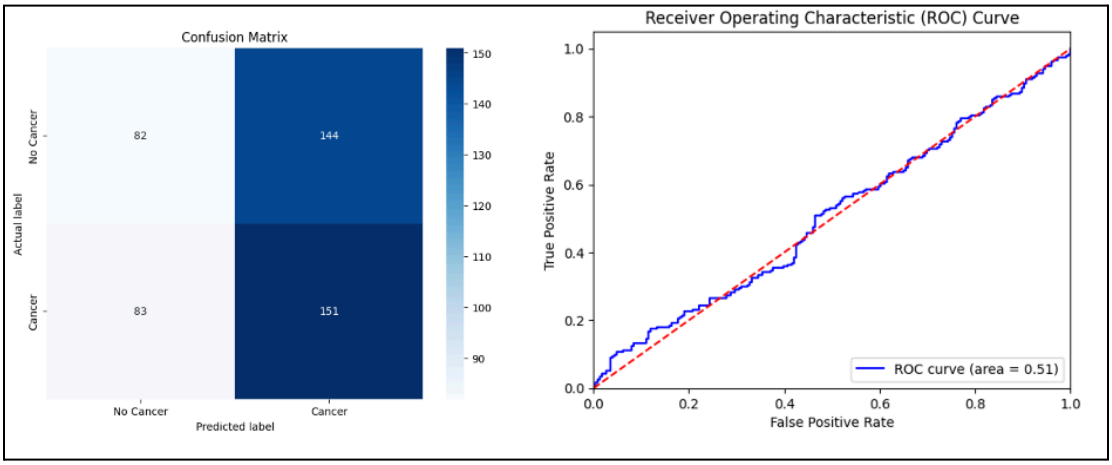


**Figure 13: InceptionV3 Results on PAD-UFES Dataset**

**DenseNet121:**

The DenseNet-121 model was evaluated on three datasets HAM10000, ISIC 2016, and PAD-UFES-20 datasets. Figures 15, 16, and 17 show the model's performance on these datasets. The model on HAM10000, showed strong benign classification with 1305 true positives and 36 false positives but it showed poor malignant detection with 5 true positives and 217 false negatives which indicates model's strong bias towards benign. The low ROC-AUC score of 0.491 reflects that the model's performance is near-random which highlights the need for improving malignant sensitivity to support reliable clinical decisions. In the ISIC 2016 dataset, benign classification was perfect with 304 true positives and 0 false positives, but malignant detection still remained weak with only 4 true positives and 71 false negative which again shows bias of the model towards benign cases. However, the 0.73 value of ROC-AUC suggests that the model has potential and with further tuning and balanced data it can perform well. For the PAD-UFES-20 dataset, the model performed more evenly by identifying 159 benign and 174 malignant cases correctly, though 67 benign and 60 malignant cases were still misclassified. The ROC-AUC score of 0.8504 indicates overall strong accuracy and better handling of this dataset. To summarise, DenseNet-121 performs well on benign cases across datasets but it lacks sensitivity for malignant detection.

Received: July 25, 2025

**International Journal of Applied Mathematics**
**Volume 38 No. 4s, 2025**
ISSN: 1311-1728 (printed version); ISSN: 1314-8060 (on-line version)

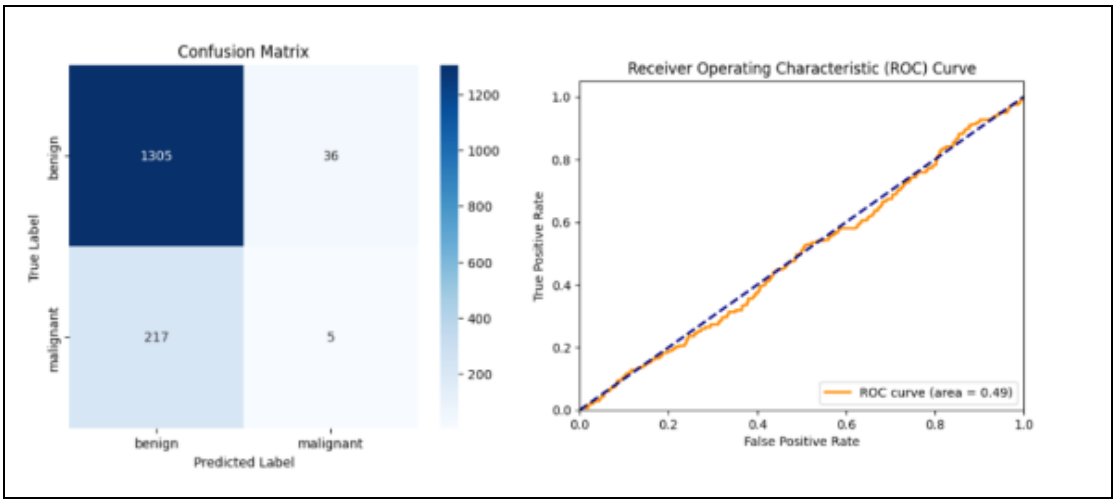


**Figure 14: DenseNet121Results on HAM10000 Dataset**

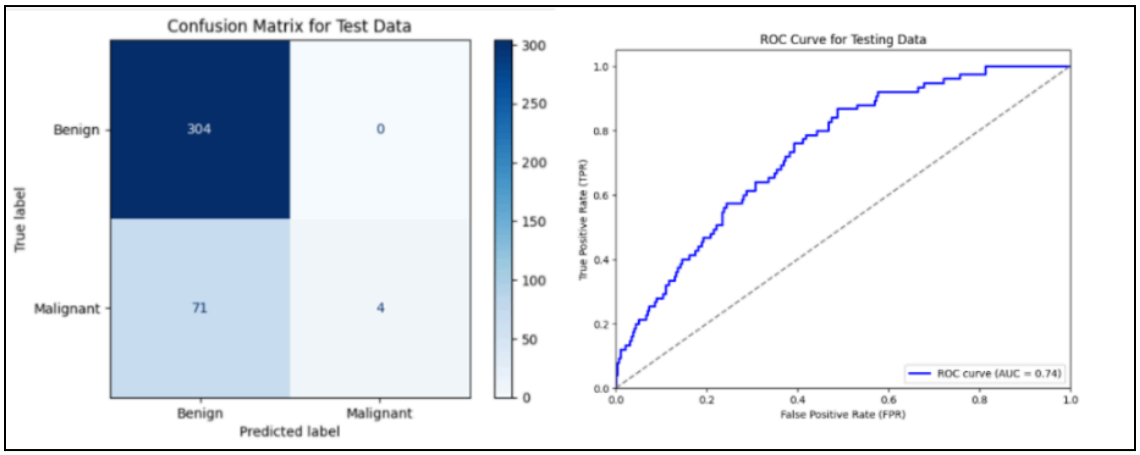


**Figure 15: DenseNet121 Results on ISIC 2016 Dataset**

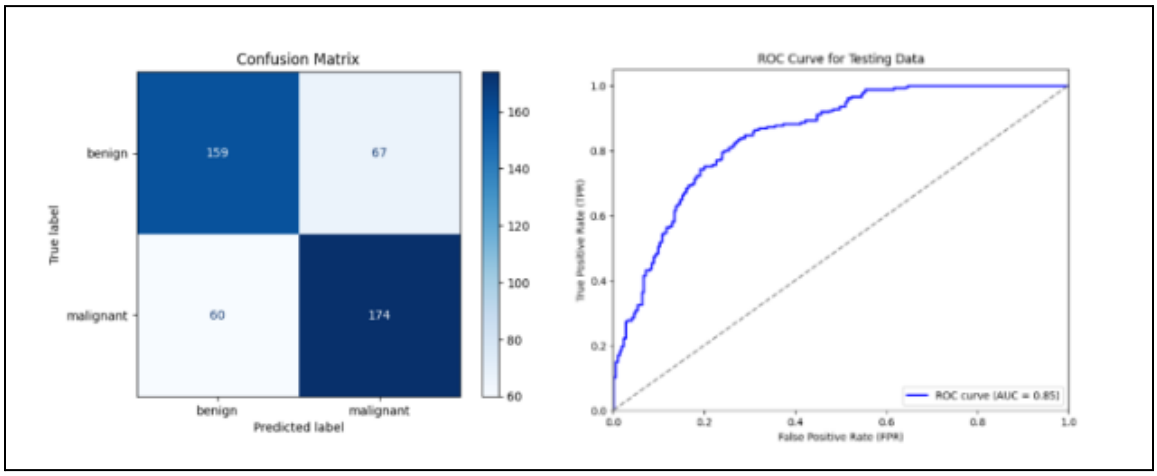


**Figure 16: DenseNet121Results on PAD-UFES-20 Dataset**

Received: July 25, 2025

**International Journal of Applied Mathematics**
**Volume 38 No. 4s, 2025**
ISSN: 1311-1728 (printed version); ISSN: 1314-8060 (on-line version)

**EfficientNetB1:**

The EfficientNetB1 achieved a test accuracy of 85.76% and an AUC score of 0.74 on the HAM10000 dataset, indicating balanced and strong classification performance. On the ISIC 2016 dataset, it reached 80.21% accuracy and AUC of 0.57, suggests moderate effectiveness but slightly lower discriminatory power. However, on PAD-UFES-20, its performance dropped significantly, with an accuracy of 52.60% and AUC of 0.49, shows challenges in handling smaller,less diverse datasets. Overall,EfficientNetB1 demonstrates good results on HAM10000 and ISIC2016 but struggles with PAD-UFES-20, which shows limited generalization across diverse datasets. To address this issue require enhanced preprocessing,feature extraction and optimization strategies. Figure 17, 18 and 19 illustrate the confusion matrices and ROC curves of EfficientNetB1 for each dataset.

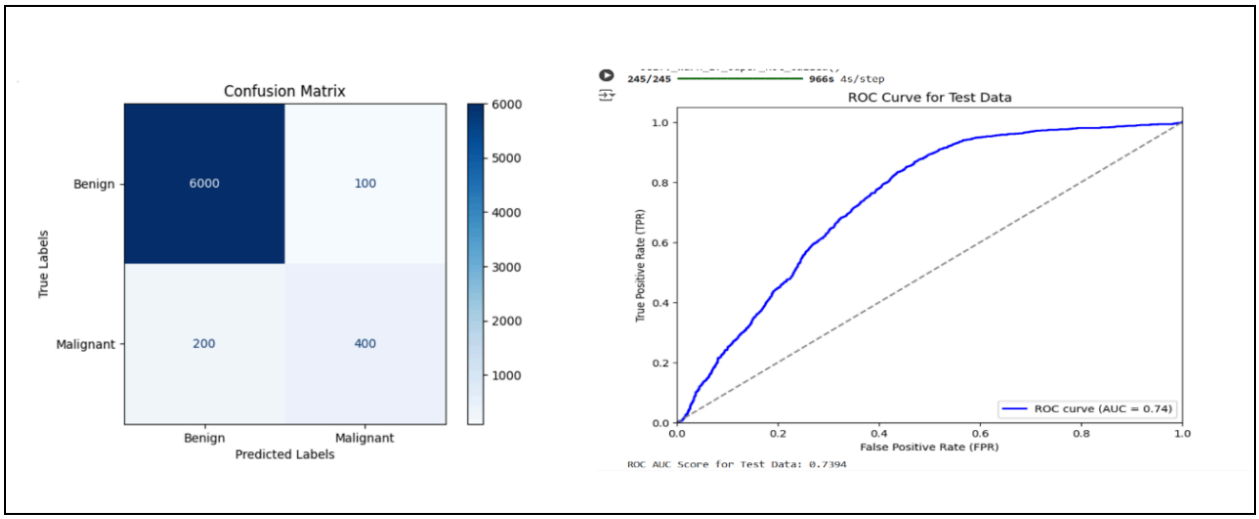


**Figure 17: EfficientNetB1 Results on HAM10000 Dataset**

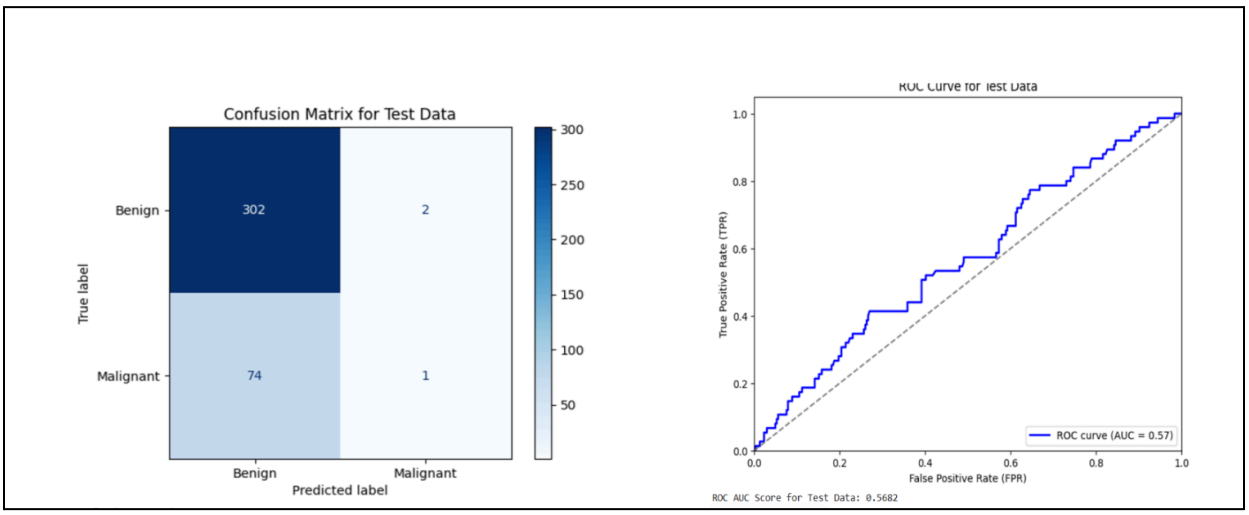


**Figure 18: EfficientNetB1 Results on ISIC 2016 Dataset**

**International Journal of Applied Mathematics**
**Volume 38 No. 4s, 2025**
ISSN: 1311-1728 (printed version); ISSN: 1314-8060 (on-line version)

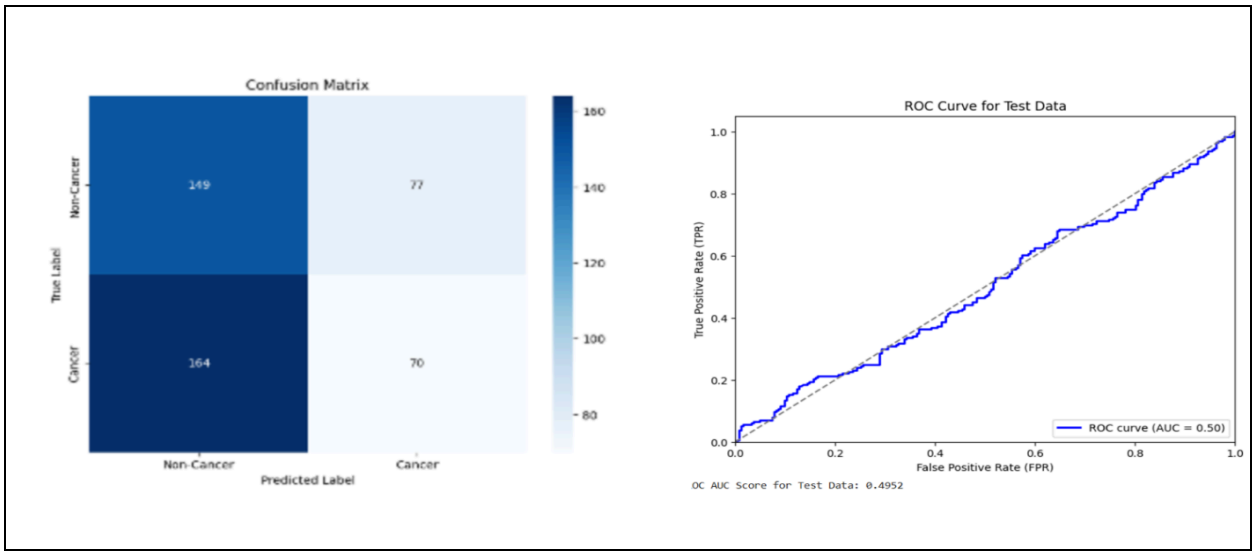


**Figure 19: EfficientNetB1 Results on PAD-UFES-20 Dataset**

**Table 2. Summary of Results**

| Model | HAM 10000 | | | ISIC 2016 | | | PAD-UFES-20 | | |
|---|---|---|---|---|---|---|---|---|---|
| | Accuracy | AUC | F1 Score | Accuracy | AUC | F1 Score | Accuracy | AUC | F1 Score |
| **VGG19** | 87.39% | 0.88 | 0.93 | 79.95 % | 0.73 | 0.89 | 60.65 % | 0.46 | 0.55 |
| **InceptionV3** | 69.24% | 0.63 | 0.69 | 83.64 % | 0.79 | 0.81 | 73.26 % | 0.51 | 0.56 |
| **DenseNet121** | 88.45% | 0.49 | 0.48 | 81.20 % | 0.73 | 0.50 | 75.96 % | 0.85 | 0.73 |
| **EfficientNetB1** | 85.76% | 0.74 | 0.80 | 80.21 % | 0.57 | 0.88 | 52.60 % | 0.50 | 0.55 |

Received: July 25, 2025

International Journal of Applied Mathematics
Volume 38 No. 4s, 2025
ISSN: 1311-1728 (printed version); ISSN: 1314-8060 (on-line version)

**Table 3. Comparison of Results**

| Model | Dataset | Accuracy | Our accuracy |
|---|---|---|---|
| **VGG19** | HAM10000 | 82% [5] | 87.39% |
| | ISIC Archive | 87% [6] | 79.95% |
| **InceptionV3** | ISIC Archive | 98% [8] | 83.64% |
| **DenseNet121** | ISIC 2018 | 81.5% [11] | 82.20% |
| **EfficientNetB1** | HAM10000 | 84.3% [13] | 85.76% |
| | ISIC Archive | 82.5% [14] | 80.21% |
| | PAD-UFES-20 | 76% [15] | 72.60% |

## V. Conclusion:

This study assessed the effectiveness of four deep learning models: VGG19, InceptionV3, DenseNet121, and EfficientNetB1, on three datasets for binary classification of skin cancer, including HAM10000, ISIC2016, and PAD-UFES-20. VGG19 had the highest performance on HAM10000 and demonstrated the best extraction of features from images, but all models had a cost associated with high computing power requirements and fine-tuning, especially with limited resources. A classification imbalance problem due mostly to benign lesions was exposed in the ISIC2016 and HAM10000 datasets (80% benign), and consequently, strong augmentation has to be incorporated into future work. EfficientNetB1 has proven to have a consistent performance metric, as well as DenseNet121 performance was attributed to its dense features from its layers, especially on the PAD-UFES-20 classification. Only EfficientNetB1 was tested temporarily due to the hardware capability; however, the study discussed the rest of the EfficientNet family of models (B0-B7). The study also acknowledges that the addition of metadata and clinical data could increase the variability and generalizability of the deep learning models. Overall, the study concluded that there are high promises and pockets for the use of deep learning to help promote clinical decision support systems for the efficient detection of skin cancers, but future work is warranted on data balance and efficiency, as well as emergent technology, for example, quantum computer technology.

Received: July 25, 2025

Volume 38 No. 4s, 2025
ISSN: 1311-1728 (printed version); ISSN: 1314-8060 (on-line version)

## VI. Future Scope

This research demonstrates the capabilities of selected deep learning models, such as VGG19, InceptionV3, DenseNet121, and EfficientNet, for assessing dermoscopic images and diagnosing skin cancer based on images alone. Future advances and explorations in multimodal image data, considered in combination with patient demographic information (age, gender, ethnicity, etc.) and patient medical information (such as family history of skin disease or other skin disorders), could improve patient skin cancer diagnosis. The downside is that a limited number of balanced public datasets available for dermoscopic images will always be a challenge, but it could be possible to advance these results through new data augmentation techniques or synthetic data via Generative Adversarial networks (GANs). If possible, model interpretability using techniques like Grad-CAM could assist in building greater trust and confidence from clinical communities to adopt these newer methods. Future investigations into either "lighter" models or model compression for real-world implementation need to be examined to facilitate deployment in resource-limited areas. Clinical trials and longitudinal studies are needed before the clinical community can feel justified in using these models in real-world clinical practice for faster and more accurate detection of skin cancers.

## References:

[1] Baghani, M., Robati, R. M., Mozafari, N., Baghani, M., Kassir, M., Sheibani, F., & Mansouri, V. (2023). “Knowledge, Attitude, and Practice toward Skin Cancer among Patients of Dermatology Clinics and Medical Students/General Practitioners.” *Journal of Skin Cancer*, *2024*(1), 9081896. https://doi.org/10.1155/2024/9081896

[2] Takiddin A, Schneider J, Yang Y, Abd-Alrazaq A, Househ M. “Artificial Intelligence for Skin Cancer Detection: Scoping Review.”, Journal of Medical Internet Research. doi: 10.2196/22934., 2021

[3] Subhayu Ghosh, Sandipan Dhar, Raktim Yoddha, Shivam Kumar, Abhinav Kumar Thakur, Nanda Dulal Jana, “Melanoma Skin Cancer Detection Using Ensemble of Machine Learning Models Considering Deep Feature Embeddings”, Procedia Computer Science, vol 235, 2024, https://doi.org/10.1016/j.procs.2024.04.284.

[4] Owida, H. A.. “Developments and Clinical Applications of Noninvasive Optical Technologies for Skin Cancer Diagnosis.”, *Journal of Skin Cancer*, *2022*(1), 9218847. doi: 10.1155/2022/9218847, 2022

[5] Irfan Ali Kandhro, Selvakumar Manickam, Kanwal Fatima, Mueen Uddin, Urooj Malik, Anum Naz, Abdulhalim Dandoush, “Performance evaluation of E-VGG19 model: Enhancing real-time skin cancer detection and classification”, Heliyon, vol. 10, doi: 10.1016/j.heliyon.2024.e31488, 2024

[6] Kiran Likhar, Dr.Sonali Ridhorkar, “Enhancing Skin Cancer Detection: A Comparative Analysis of Models with VGG-16, VGG-19, and Inception V3”, International Journal of Intelligent Systems and Applications in Engineering, vol. 12, 2024.

[7] Bansal, M., Kumar, M., Sachdeva, M., et al. “Transfer learning for image classification using VGG19: Caltech-101 image data set”, Journal of Ambient Intelligence and Humanized Computing, vol. 14, pp. 3609–3620, doi: 10.1007/s12652-021-03488-z., 2023

Received: July 25, 2025

Volume 38 No. 4s, 2025
ISSN: 1311-1728 (printed version); ISSN: 1314-8060 (on-line version)

[8] Ehsan Bazgir, Ehteshamul Haque, Md. Maniruzzaman, and Rahmanul Hoque, “Skin cancer classification using Inception Network”, World Journal of Advanced Research and Reviews, vol. 21, pp. 839-849, doi: 10.30574/wjarr.2024.21.2.0500., 2024
[9] Alanazi, Saad Awadh, "Melanoma Identification Through X-ray Modality Using Inception-v3 Based Convolutional Neural Network", Computers, Materials and Continua, vol. 72, pp. 37-55, doi: 10.32604/cmc.2022.020029., 2022
[10] Bhavya Sai, Narasimha Rao, Ramya, Sujana Sree, Anuradha, “Classification of skin cancer images using TensorFlow and inception v3”, International Journal of Engineering & Technology, vol. 7, pp. 717-721, doi: 10.14419/ijet.v7i2.7.10930., 2018
[11] Rashid H, Asjid Tanveer M, Khan HA, “Skin Lesion Classification Using GAN-based Data Augmentation” 41st Annual International Conference of the IEEE Engineering in Medicine & Biology Society (EMBC), pp. 916–919, 2019
[12] Alfi IA, Rahman MM, Shorfuzzaman M, Nazir A, “A Non-Invasive Interpretable Diagnosis of Melanoma Skin Cancer Using Deep Learning and Ensemble Stacking of Machine Learning Models” Diagnostics, vol. 12, Issue 3, 2022
[13] Tajerian, A., Kazemian, M., Tajerian, M., Akhavan Malayeri, A., “Design and validation of a new machine-learning-based diagnostic tool for the differentiation of dermatoscopic skin cancer images”, PLoS One, vol. 18, pp. 0284-437, doi: https://doi.org/10.1371/journal.pone.0284437, 2023.
[14] Kanchana, K., Kavitha, S., Anoop, K.J., Chinthamani, B., “Enhancing skin cancer classification using efficient net b0-b7 through convolutional neural networks and transfer learning with patient-specific data”, Asian Pacific Journal of Cancer Prevention, APJCP, vol. 25, pp. 17-95, doi: https://doi.org/10.31557/APJCP.2024.25.5.17-95, 2024
[15] Khan, I.U., Aslam, N., Anwar, T., Aljameel, S.S., Ullah, M., Khan, R., Rehman, A. and Akhtar, N., “Remote diagnosis and triaging model for skin cancer using EfficientNet and extreme gradient boosting”, Complexity, vol. 2021(1), pp. 559-1614, doi: https://doi.org/10.1155/2021/5591614, 2021

Received: July 25, 2025